Molecular Therapy
Oncolytics
Original Article

Claudin18.2 bispecific T cell engager armed oncolytic virus enhances antitumor effects against pancreatic cancer

Shiyu Liu,[1,2,3,6] Fan Li,[2,3,6] Li Deng,[3,6] Qiongqiong Ma,[2,3] Wenyi Lu,[4] Zhuoqian Zhao,[1,2,3] Huanzhen Liu,[1] Yixuan Zhou,[5] Manli Hu,[1] Hui Wang,[3] Yingbin Yan,[5] Mingfeng Zhao,[4] Hongkai Zhang,[1,2,3] and Mingjuan Du[1]

[1]Shanghai Institute for Advanced Immunochemical Studies, ShanghaiTech University, Shanghai 201210, China; [2]State Key Laboratory of Medicinal Chemical Biology, College of Life Sciences and Frontiers Science Center for Cell Responses, Nankai University, Tianjin 300071, China; [3]Beijing Institute of Biological Products Company Limited and CNBG-Nankai University Joint Research and Development Center, Beijing 100176, China; [4]Department of Hematology, Tianjin First Central Hospital, Tianjin 300192, China; [5]Department of Oromaxillofacial-Head and Neck Surgery, Tianjin Stomatological Hospital, Tianjin 300041, China

Bispecific T cell engagers (BiTEs) represent a promising immunotherapy, but their efficacy against immunologically cold tumors such as pancreatic ductal adenocarcinoma remains unclear. Oncolytic viruses (OVs) can transform the immunosuppressive tumor microenvironment into the active state and also serve as transgene vectors to selectively express the desired genes in tumor cells. This study aimed to investigate whether the therapeutic benefits of tumor-targeting Claudin18.2 BiTE can be augmented by combining cancer selectively and immune-potentiating effects of OVs. Claudin18.2/CD3 BiTE was inserted into herpes simplex virus type 1 (HSV-1) to construct an OV-BiTE. Its expression and function were assessed using reporter cells and peripheral blood mononuclear cell (PBMC) co-culture assays. Intratumoral application of OV-BiTE restrained tumor growth and prolonged mouse survival compared with the unarmed OV in xenograft models and syngeneic mice bearing CLDN18.2-expressing KPC or Pan02 pancreatic cancer cells. Flow cytometry of tumor-infiltrating immune cells suggested both OV-BiTE and the unarmed OV remodeled the tumor microenvironment by increasing CD4+ T cell infiltration and decreasing regulatory T cells. OV-BiTE further reprogrammed macrophages to a more pro-inflammatory antitumor state, and OV-BiTE-induced macrophages exhibited greater cytotoxicity on the co-cultured tumor cell. This dual cytotoxic and immunomodulatory approach warrants further development for pancreatic cancer before clinical investigation.

INTRODUCTION

Pancreatic ductal adenocarcinoma (PDAC) is one of the most lethal solid tumors, with 466,003 deaths worldwide in 2020.[1,2] Conventional chemotherapy and radiation do not significantly improve life expectancy, and immunotherapy has not been proved effective to date.[3] This lack of success is attributed to the immunosuppressive tumor microenvironment (TME) and the presence of a dense extracellular matrix, both of which contribute to resistance against immunotherapies.[4]

To address these challenges, bispecific T cell engagers (BiTEs) have emerged as a promising immunotherapy approach. BiTEs are made of two scFv with one scFv targeting a tumor-specific antigen on tumor cells and the other targeting CD3 on T cells. BiTEs can redirect T cells to recognize and eliminate tumor cells effectively. Claudin 18.2 is highly expressed in a significant proportion of gastric cancers as well as pancreatic and esophageal adenocarcinoma. Therefore, it is an ideal target for antibody or chimeric antigen receptor T (CAR-T) cell-based therapy.[5–8] However, inefficient T cell trafficking into tumors, the immunosuppressive TME, and potential on-target off-tumor toxicity of certain bispecific antibodies have hindered the effectiveness of BiTE therapies in pancreatic cancer treatment.[9] These shortcomings could be overcome by using vector delivery, such as oncolytic viruses (OVs).

Growing insights into antitumor immunity and the TME have inspired the development of oncolytic virotherapy.[10–16] OVs can convert immunologically cold tumors into hot ones by activating innate and adaptive immunity. Moreover, intratumoral delivery of transgenes by OV enables gene expression *in situ*, which is important for some immune-stimulating proteins because the systemic administration of these immune modulators is associated with severe adverse effects.[17] Talimogene laherparepvec (T-VEC) represents a major advance as the first US Food and Drug Administration

Received 26 March 2023; accepted 22 August 2023;
https://doi.org/10.1016/j.omto.2023.08.011.

[6]These authors contributed equally

Correspondence: Yingbin Yan, Department of Oromaxillofacial-Head and Neck Surgery, Tianjin Stomatological Hospital, Tianjin 300041, China.
E-mail: yingbinyan@qq.com
Correspondence: Mingfeng Zhao, Department of Hematology, Tianjin First Central Hospital, Tianjin 300192, China.
E-mail: mingfengzhao@sina.com
Correspondence: Hongkai Zhang, Shanghai Institute for Advanced Immunochemical Studies, ShanghaiTech University, Shanghai 201210, China.
E-mail: hongkai@nankai.edu.cn
Correspondence: Mingjuan Du, Shanghai Institute for Advanced Immunochemical Studies, ShanghaiTech University, Shanghai 201210, China.
E-mail: dumj@shanghaitech.edu.cn

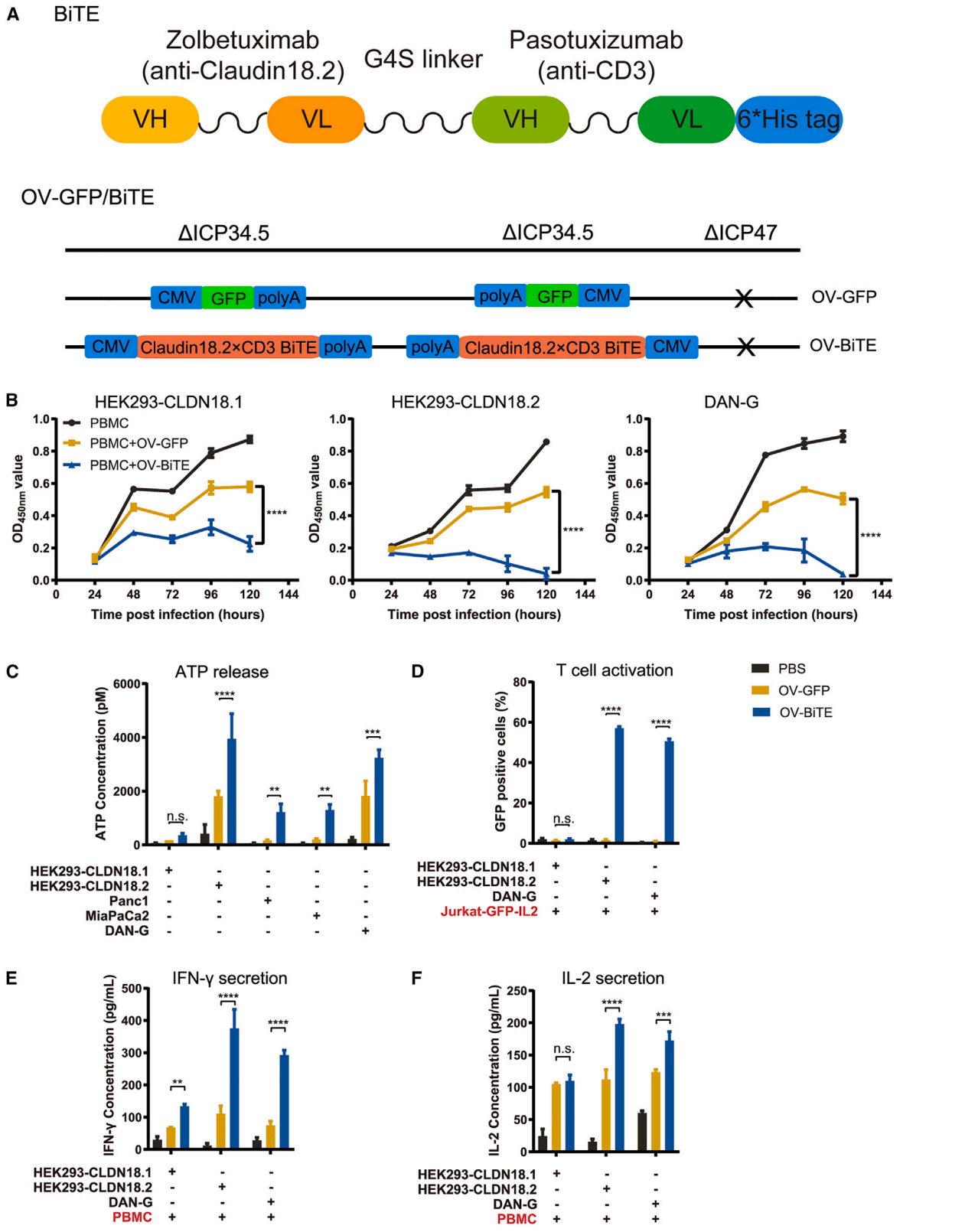

(legend on next page)

(FDA)-approved oncolytic immunotherapy.[18] T-VEC is an engineered herpes simplex virus type 1 (HSV-1) with deletions of ICP34.5 and ICP47 genes along with the insertion of granulocyte-macrophage colony-stimulating factor (GM-CSF) to enhance systemic antitumor immunity. In a phase III trial for advanced melanoma, T-VEC as monotherapy demonstrated improved durable response rates, overall response, and median overall survival compared to GM-CSF alone.[19] Moreover, T-VEC exhibits a manageable safety profile with minimal serious adverse events. T-VEC is now under clinical evaluation for multiple solid tumors, including pancreatic ductal adenocarcinoma. Additionally, LOAd703, a TMZ-CD40L/4-1BBL-armed oncolytic adenovirus, has shown promising efficacy signals in early pancreatic cancer trials when combined with chemotherapy.[20] A phase I/II study revealed favorable objective response and safety for LOAd703 with nab-paclitaxel and gemcitabine.

In this study, we engineered and characterized a novel Claudin18.2/CD3 BiTE-armed oncolytic HSV (OV-BiTE) against pancreatic cancer by combining the targeted approach of BiTE therapy with the immunostimulatory effects of oncolytic virotherapy. Our results suggested OV-BiTE selectively infected and killed Claudin18.2-expressing tumors and showed enhanced cytotoxicity when co-cultured with peripheral blood mononuclear cells (PBMCs) versus the control virus. In subcutaneous syngeneic models, OV-BiTE inhibited tumor growth and prolonged survival compared to the control virus. Flow cytometry of tumor-infiltrating lymphocytes demonstrated OV-BiTE increased CD4+ T cells and shifted macrophages from M2 to M1 phenotype compared to PBS or control virus. Isolated tumor-associated macrophages (TAMs) from OV-BiTE-treated mice also showed enhanced tumor cell cytotoxicity in co-cultures. Our study provides preclinical proof of concept for a novel immunotherapeutic approach against PDAC.

RESULTS

Generation and characterization of Claudin18.2 BiTE-armed oncolytic HSV

To generate OV-BiTE, the Claudin18.2/CD3 BiTE expression cassette was inserted into the backbone of ICP34.5 and ICP47 double-deleted oncolytic HSV-1 (Figure 1A). Vero cells infected with OV-BiTE secreted BiTE molecules, as determined by pull-down assay (Figure S1A). The pancreatic cancer cells, Panc-1, Miapaca-2, and DAN-G, were infected with either OV-GFP or OV-BiTE, and OV-BiTE exerted similar replication capability and tumoricidal activity compared with OV-GFP (Figure S1B).

OV-BiTE enhanced the antitumor effect against Claudin18.2-positive cells when co-cultured with PBMCs

The antitumor efficacy and specificity of Claudin18.2 were evaluated. In co-culture with PBMCs, HEK293-GFP-Claudin18.1, HEK293-GFP-Claudin18.2, and DAN-G cells, which expressed a higher level of Claudin18.2 protein compared with MiaPaca-1 and Panc1 (Figure S2), were infected with OV-BiTE or OV-GFP. The viability of OV-BiTE-infected DAN-G and HEK293-GFP-Claudin18.2 cells was dramatically decreased compared with that of DAN-G and HEK293-GFP-Claudin18.2 cells infected by OV-GFP or HEK293-GFP-Claudin18.1 infected by OV-BiTE (Figure 1B). In co-culture with PBMCs, Claudin18.2-positive cells infected with OV-BiTE released a higher level of ATP compared to OV-GFP (Figure 1C), indicating OV-BiTE might also induce immunogenic tumor cell death in addition to tumor cell death resulting from OV infection.

The activation of T cells mediated by OV-BiTE-infected Claudin18.2 tumor was assessed using Jurkat-GFP-IL2 reporter cells that express GFP upon activation of T cells. In co-culture with the Jurkat-based reporter cells, the OV-BiTE pre-infected DAN-G and HEK293-GFP-Claudin18.2 cells stimulated the reporter cells more than the OV-BiTE pre-infected HEK293-GFP-Claudin18.1 cells (Figure 1D). Moreover, the OV-BiTE-infected Claudin18.2-positive cells exhibited a potent stimulating activity on PBMCs as observed by the high levels of interferon-γ (IFN-γ) and interleukin-2 (IL-2) in the supernatant of co-cultured virus-infected tumor cells and PBMCs (Figures 1E and 1F).

OV-BiTE inhibited tumor growth in the DAN-G cell xenograft mouse model

A DAN-G cell xenograft mouse model was established to study the antitumor efficacy of OV-BiTE (Figure 2A). The tail vein injection of PBMCs alone had a negligible effect on tumor growth compared with vehicle treatment (Figure 2B). The combination of OV-GFP and PBMCs slightly inhibited tumor growth compared to PBMC alone. In contrast, OV-BiTE administration significantly enhanced the antitumor efficacy of PBMCs and delayed tumor growth compared with the combination of PBMCs and OV-GFP ($p < 0.0001$).

The limited infiltration of CD3 cells into the tumor partially explained the modest efficacy, and OV-BiTE significantly increased the infiltration of T cells into the tumor and resulted in extensive areas of tumor cell necrosis, demonstrated by immunohistology staining with anti-CD3 antibody and picrosirius red staining (Figure 3). An additional animal model that could recapitulate the TME of PDAC was warranted.

OV-BiTE inhibited tumor growth in syngeneic pancreatic cancer mouse models

A mouse KPC cell line expressing human Claudin 18.2 (KPC-Claudin18.2) was first established using the modified HSV-1-susceptible mouse KPC cells. OV-BiTE exhibited a similar replication capacity compared to OV-GFP in KPC-Claudin18.2 cells but significantly

Figure 1. Lytic activity and T cell engagement by OV-BiTE versus control virus

(A) Schematic of BiTE targeting Claudin18.2 and CD3ε, and HSV-1-based OV encoding BiTE or GFP. (B) Cell viability of HEK293 cells expressing Claudin18.1 or Claudin18.2 and DAN-G cells after infection with OV-BiTE or OV-GFP and co-culture with PBMCs. (C) ATP release by infected tumor cells co-cultured with PBMCs. (D) Activation of Jurkat-GFP-IL2 reporter cells by infected tumor cells. (E) IFN-γ and (F) IL-2 production by PBMCs co-cultured with infected tumor cells. Data were analyzed using one-way ANOVA with Dunnett tests or two-way ANOVA with Sidak's tests. ns, not significant. *$p < 0.05$, **$p < 0.01$, ***$p < 0.001$, and ****$p < 0.0001$.

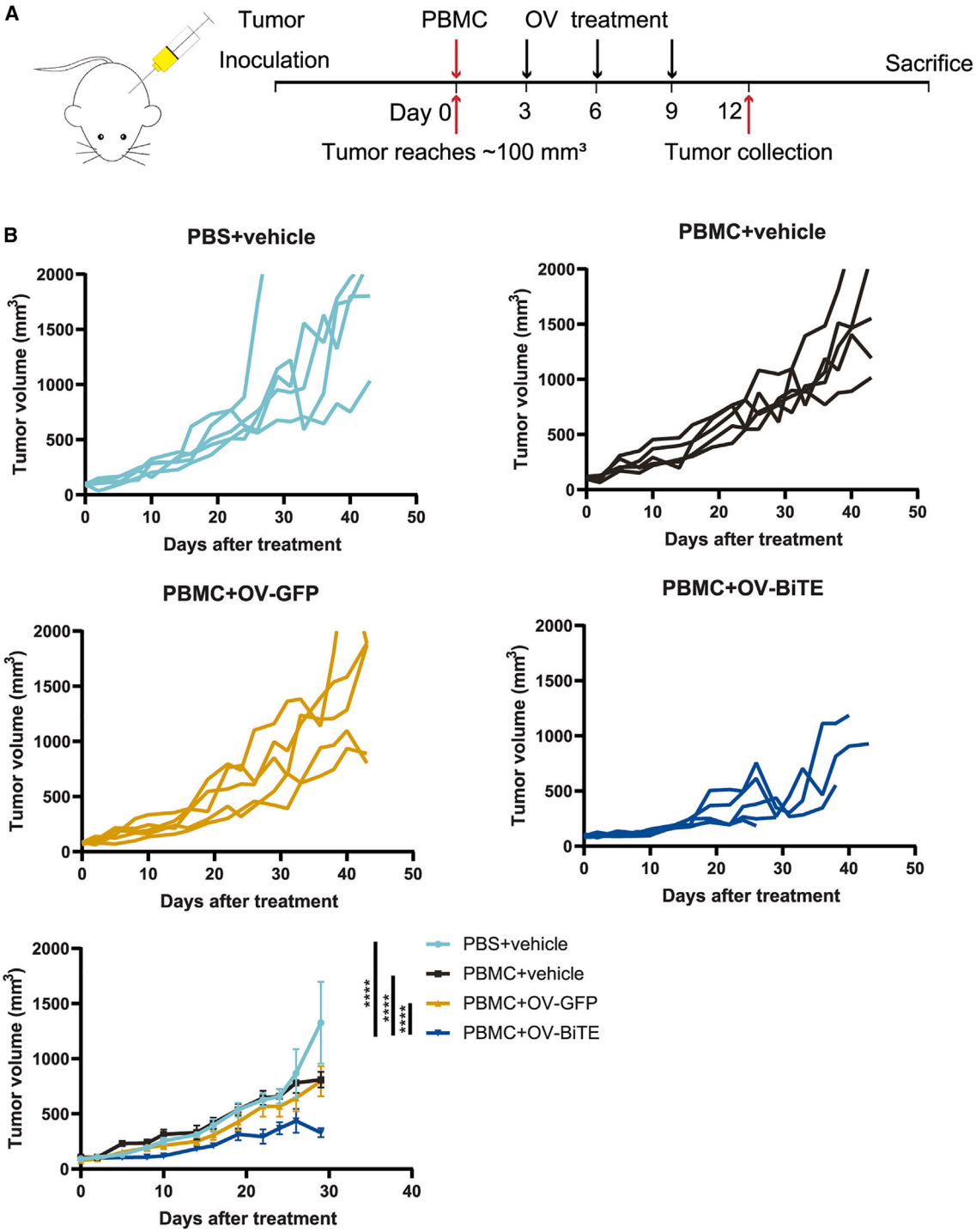

Figure 2. Tumor growth inhibition by OV-BiTE treatment in DAN-G xenograft model

(A) Treatment schedule in subcutaneous DAN-G pancreatic tumor model. (B) Tumor growth curves of mice treated with OV-BiTE, OV-GFP, or vehicle control in combination with PBMCs. Data were analyzed using two-way ANOVA with Sidak's tests. ****$p < 0.0001$.

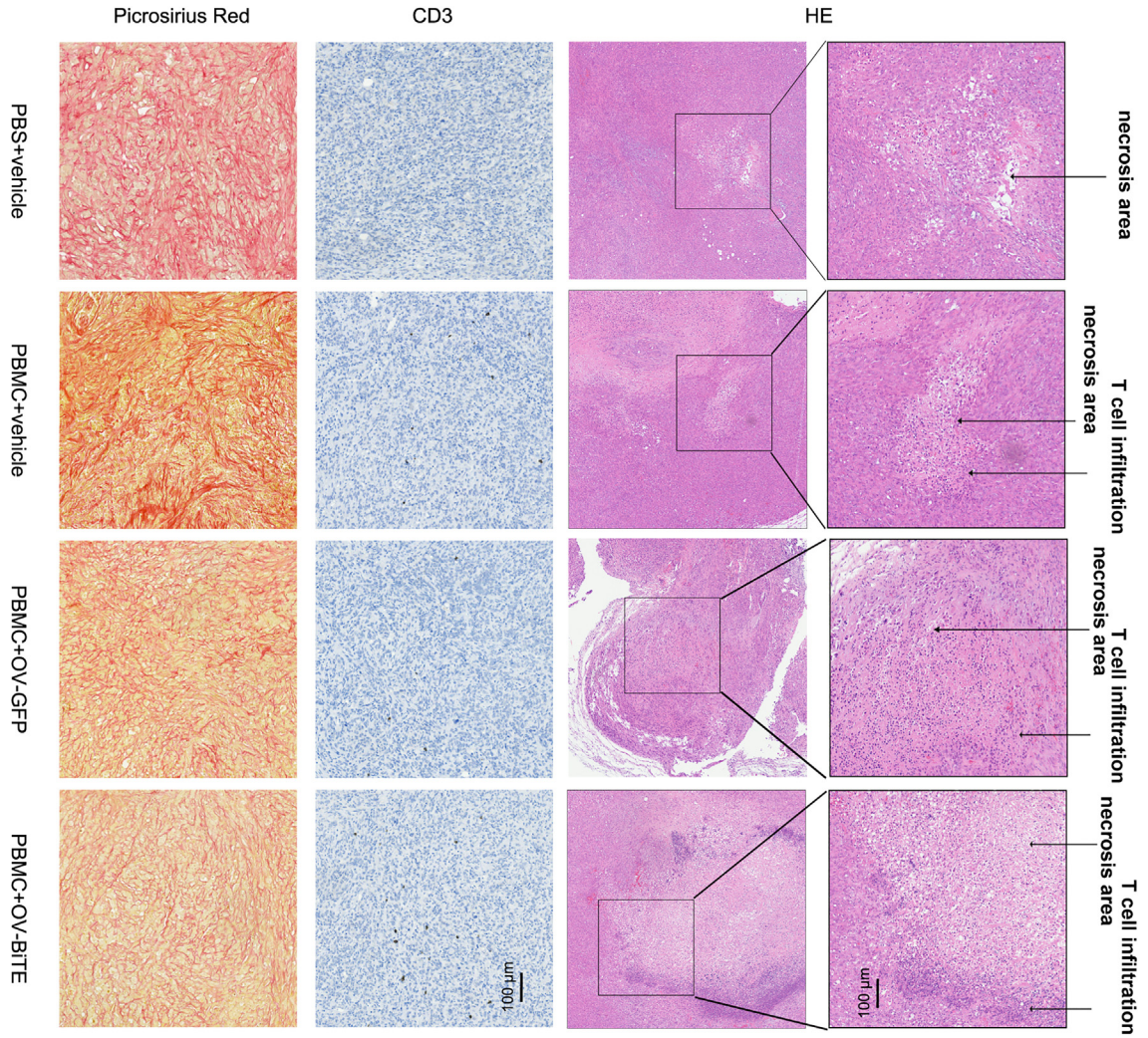

Figure 3. Histological staining of DAN-G tumors after treatment

Representative images of H&E staining, picrosirius red staining, and anti-CD3 IHC from tumors of mice treated with OV-BiTE, OV-GFP, or vehicle control in combination with PBMCs.

inhibited cell growth in co-culture with mouse spleen lymphocytes (Figures 4A and 4B).

A syngeneic pancreatic cancer mouse model was then established by inoculating KPC cells into CD3ε humanized mice as previously described.[21,22] This model showed intense desmoplasia and an immunosuppressive environment that recapitulated the TME of PDAC patients.[22] Tumor-bearing mice were treated with OV-GFP or OV-BiTE (Figure 4C). Compared with the PBS control, intratumoral administration of OV-GFP slightly inhibited tumor growth while OV-BiTE significantly inhibited tumor growth (Figure 4D). Similar results were observed regarding survival in mice (Figure 4E). No survival benefit was observed in OV-GFP-treated mice with a similar median survival time compared to control mice (25.5 vs. 26 days), although the mean survival time of OV-GFP treated mice was longer than the control mice (29.2 vs. 24.2 days) and two out of six mice survived for a relatively long time. In contrast, OV-BiTE significantly prolonged the survival of the mice, with a median survival time of 42 days and a mean survival time of 44.5 days. All treatments were well-tolerated with no significant weight loss or other signs of distress. No liver/kidney toxicity was observed upon treatment by OV-BiTE as assessed by the histology staining of the liver and kidney and biochemical blood test (Figure S3). The intense desmoplasia in TME of the KPC model might affect the OV spread and subsequently affects its therapeutic effects, especially the unarmed OV. We then established another syngeneic pancreatic cancer mouse model with less stromal desmoplasia by inoculating Pan02_HVEM_Claudin18.2 cells into CD3ε humanized mice, in which OV-GFP has been reported to exert antitumor effects in our previous work.[23] In Pan02 model mice, compared with the PBS control, intratumoral administration of OV-GFP significantly

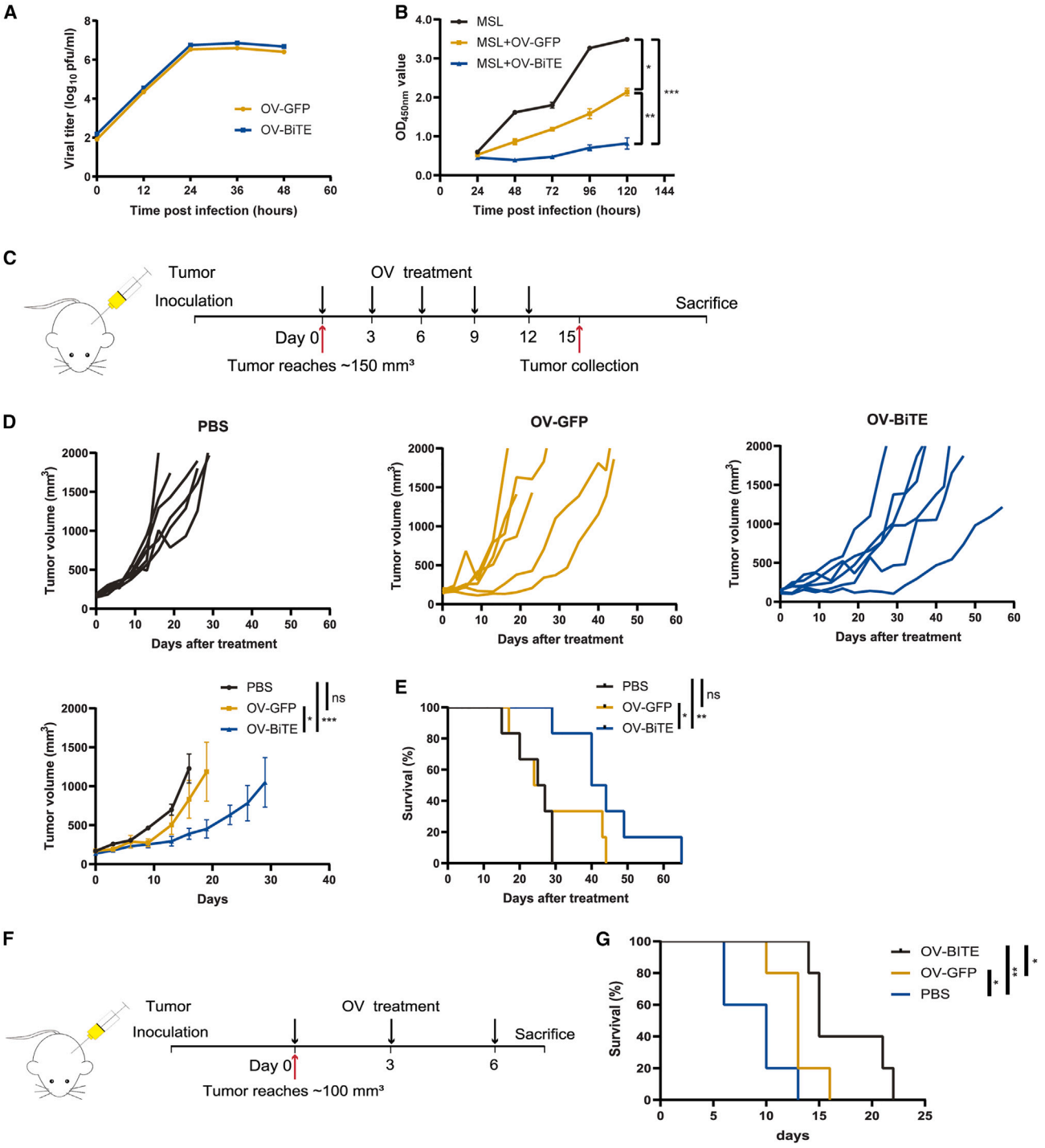

Figure 4. Antitumor effects of OV-BiTE in pancreatic cancer models

(A) Viral replication kinetics in KPC cells. (B) Cytotoxicity against KPC cells after co-culture with spleen lymphocytes of CD3E humanized mice. (C) Treatment schedule for KPC syngeneic model. (D) Tumor growth curves for KPC syngeneic model. (E) Survival curves in the KPC model. (F) Treatment schedule for the Pan02 model. (G) Survival curves in the Pan02 model. MSL, mouse spleen lymphocytes. Data were analyzed using two-way ANOVA with Sidak's tests. Animal survival was plotted using Kaplan–Meier curves and compared using the log-rank test. ns, not significant. *$p < 0.05$, **$p < 0.01$, and ***$p < 0.001$.

improved mouse survival, with a median survival time of 13 vs. 10 days and mean survival time of 13 vs. 9 days, and OV-BiTE further significantly prolonged mouse survival with a median survival time of 15 days and a mean survival time of 17.4 days (Figures 4F and 4G).

Effects of OV treatment on TME

To explore the mechanism underlying OV-BiTE treatments, tumor-infiltrating lymphocytes were analyzed by flow cytometry 3 days after the last treatment. Both OV-GFP and OV-BiTE increased the proportion of conventional CD4+ T cells among all immune cells, with the highest increase in OV-BiTE treatment, although the comparison between the two OV groups was not statistically significant (Figure 5A). The increase of CD4+ T cells in the OV-BiTE group was also demonstrated by multiplex immunohistochemistry (mIHC) staining of tumor sections (Figure S4). The proportion of CD8+ T cells among CD45+ immune cells did not change after OV treatment (Figure 5B). Regulatory T cells (Tregs) were dramatically decreased but no significant difference was observed between OV-GFP and OV-BiTE groups (Figure 5C). CD8+ T cells with positive lymphocyte activation gene 3 (LAG-3) or programmed cell death protein 1 (PD-1) expression were decreased, while those with positive Granzyme B (GzmB) expression were increased by OV treatment, and OV-GFP and OV-BiTE exerted similar effects (Figures 5D–5F). OV treatment did not alter the number of TAMs, characterized as CD11b+ F4/80+ (Figure 5G). The pro-inflammatory M1-like macrophages, as indicated by the inducible nitric oxide synthase (iNOS) expression, were significantly increased in the OV-BiTE group compared with PBS control and OV-GFP groups, whereas the anti-inflammatory M2-like macrophages (CD206+) were decreased (Figures 5H and 5I). The results revealed a possible shift toward potentiating macrophages from immunosuppressive to pro-inflammatory. To evaluate and compare the tumor-killing potential of TAMs and T cells from KPC mice treated with OV-GFP or OV-BiTE, TAMs were isolated from the tumors of treated mice, while splenocytes from a freshly sacrificed mice served as effector T cells. Claudin18.2-expressing KPC tumor cells were co-cultured with TAMs and splenocytes at a 1:5:1 ratio for 3 days, and cell viability was determined by the Cell Counting Kit-8 (CCK8) assay. The results suggested that TAMs induced by OV-BiTE had the highest tumor-killing effects in co-culture with T cells compared with that in PBS and OV-GFP groups, demonstrated by the lowest cell viability (Figure 5J).

DISCUSSION

In this study, an armed HSV-1-based OV was developed to encode Claudin18.2 targeting BiTE to treat pancreatic cancer. This approach was designed to combine the direct oncolytic effect of the OV with the immune-stimulating activity mediated by both the OV and BiTE. The BiTE-armed OV can effectively delay tumor growth, resulting in extended survival time in the syngeneic KPC mouse model.

OVs that express various kinds of BiTE have been evaluated in previous studies. An oncolytic vaccinia virus encoding an EphA2-targeting BiTE resulted in an enhanced antitumor response in an A549 subcutaneous xenograft model.[24] Similarly, the combined delivery of an EGFR-targeting BiTE-armed adenovirus with PBMCs enhanced the antitumor efficacy achieved by either component in xenograft models. Antitumor efficacy of oncolytic measles viruses encoding BiTE was assessed in a syngeneic mouse model bearing MC38 or B16 tumor cells.[25–27] The combination of BiTE-expressing OV armed with CAR-T cell therapy enabled the dual targeting of two tumor antigens of heterogeneous solid tumors.[13,28] The focus of these pioneering studies was the effect of the OV on T cell infiltration and activation, while the effect on the other components of the TME, such as myeloid-derived immune cells and stromal fibroblast cells, was not studied. In this study, the BiTE-encoding OV was at least equally important for activating non-T cells compared with T cells. A comprehensive study of the mechanism of action of BiTE-armed OV on the tumor immune microenvironment and stromal dysplasia is needed before the clinical investigation of this promising modality.

Flow cytometry of tumor-infiltrating immune cells showed that BiTE-armed oncolytic HSV (OV-BiTE) and control virus (OV-GFP) increased CD4+ T cell infiltration and decreased Tregs compared to PBS. Neither virus altered CD8+ T cell proportions, although they did appear to reduce exhaustion markers such as LAG-3 and PD-1 and increase activation markers such as GzmB on CD8+ cells. This suggests the viruses help reinvigorate existing intratumoral CD8+ T cell function. However, OV-BiTE uniquely shifted macrophages from an M2 to an M1 phenotype. M1 macrophages play a pro-inflammatory, antitumor role. This was further shown by the enhanced tumoricidal activity of macrophage and T cell mixtures upon OV-BiTE treatment, confirming they acquire anti-cancer functions. Repolarization of TAMs from a pro-tumorigenic M2 toward a more pro-inflammatory M1 phenotype was also observed during EnAd-SA-FAP-BiTE treatment,[29] and TAMs have been identified as a target when developing BiTE-armed OVs.[30]

There were several shortages in our articles. First, the models used were limited to subcutaneous xenografts or syngeneic pancreatic cancer. Testing in additional models such as patient-derived xenografts or genetically engineered mouse models could better replicate pancreatic cancer complexity. Second, the specific mechanisms underlying the observed TME changes remain to be fully elucidated. More in-depth analysis of immune cell subsets and functional effects is needed. Understanding factors driving the increased M1/decreased M2 macrophage ratio could guide strategies to further relieve immunosuppression.

Another limitation of this study is that the BiTE-armed OV did not further improve T cell infiltration compared to the unarmed virus in the syngeneic model. The BiTE provides localized T cell activation and redirected tumor cell cytotoxicity, but it may be limited by inadequate T cell infiltration. Evaluation of viral persistence suggested active oncolytic HSV replication at day 13 (1 day after the last treatment), which cleared by day 16 (Figure S5). While the oncolytic viral replication appears transient, we expect infected cells likely continue to express the encoded BiTE for a period after initial infection and lysis. However, considering the short half-life of BiTE proteins, sustained production may be limited. In the future, we will also engineer the virus to encode a longer-acting BiTE derivative, such as a BiTE-monovalent

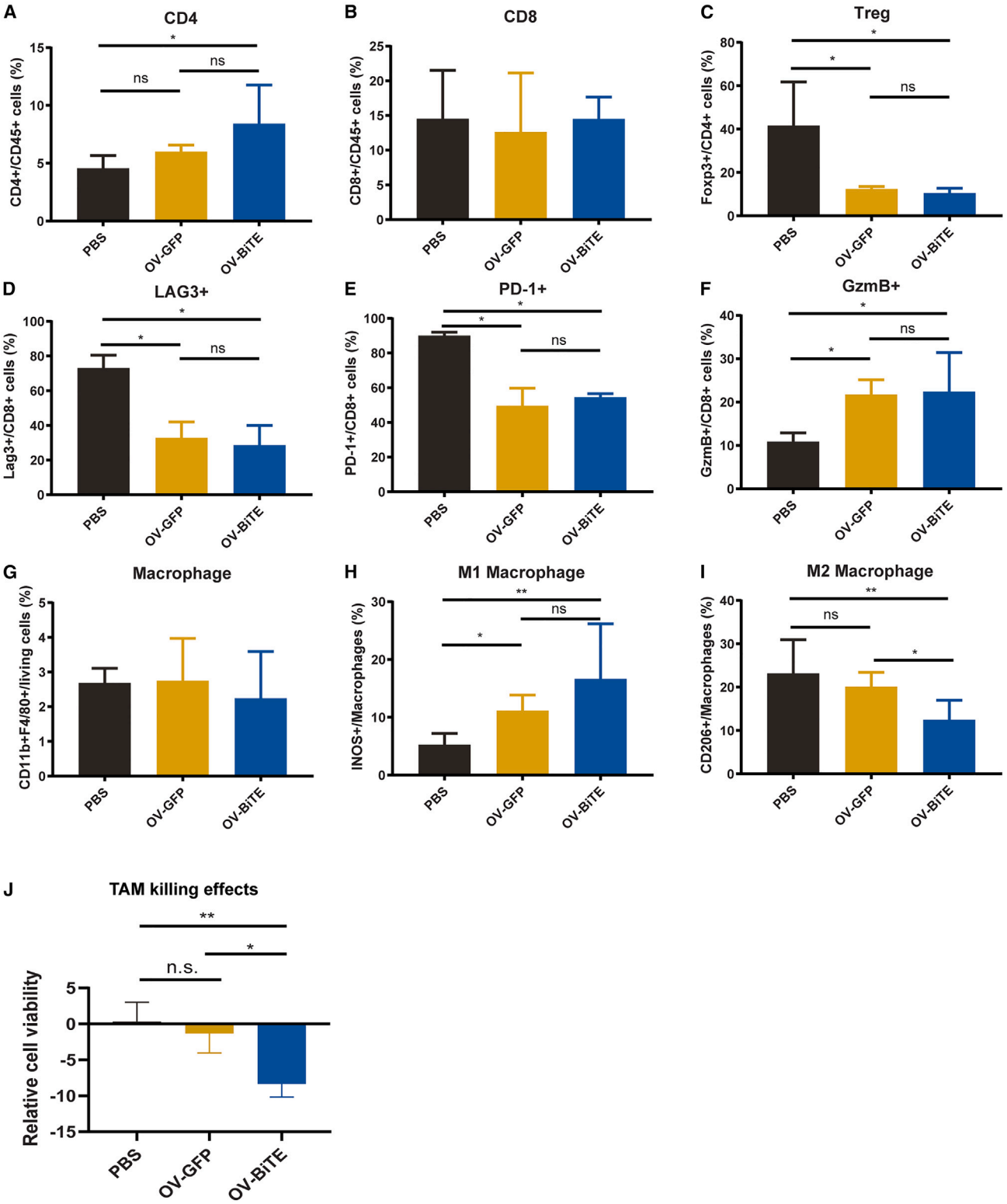

Figure 5. Analysis of tumor-infiltrating leukocytes and TAM cytotoxicity after OV treatment

(A–I) Flow cytometry quantifying infiltrating immune cell populations in KPC tumors at 3 days after the last treatment. (J) Co-culture assay measuring cytotoxicity of TAMs isolated from treated tumors against KPC cells by the CCK-8 method. Data were analyzed using one-way ANOVA with Dunnett tests or two-way ANOVA with Sidak's tests. ns, not significant. *$p < 0.05$ and **$p < 0.01$.

Fc fusion, which could potentially extend the duration of BiTE signaling after initial viral delivery and cell infection. Prolonging BiTE exposure could help maintain T cell stimulation against infected tumor cells and their released antigens after viral clearance. In addition, a combination with an alternative armed virus such as C-C motif chemokine ligand 5 (CCL5)-armed oncolytic HSV, which can attract T cells and natural killer (NK) cells to infiltrate into tumors, might be an efficient way to enhance the antitumor effects of OV-BiTE. Unexpectedly, the combination of OV-BiTE with CCL5-armed oncolytic HSV was tested but no additional effect was observed (data not shown). The result suggested that other factors, such as the physical barriers from stroma/fibrosis or other immunosuppressive mechanisms, affect the efficacy of BiTE-armed OV.

In conclusion, we combined the therapeutic benefits of tumor-targeting BiTE with the cancer-selecting and immune-potentiating effects of OV to treat pancreatic cancer. The armed OV therapy not only redirects T cells to kill cancer cells but also potentiates the antitumor efficacy of T cell-centered therapies such as BiTE by remodeling the TME.

MATERIALS AND METHODS

Cells

Vero, PANC-1, and MiaPaCa-2 cells were originally obtained from ATCC (VA, USA). The murine pancreatic tumor KPC cell line was derived from pancreatic tumors of C57BL/6-*Trp53*$^{em4(R172H)}$*Kras*$^{em4(LSL-G12D)}$Tg(Pdx1-cre) Smoc mice. The murine pancreatic tumor Pan02_HVEM cell line was established previously. The mammalian cell expression plasmid pCDH-Claudin18.1 or pCDH-Claudin18.2 was transfected into HEK293FT, Pan02_HVEM, or KPC cells and these cells were selected in the presence of puromycin to construct Claudin-expressing cells. These cells were cultured in DMEM supplemented with 10% fetal bovine serum (FBS) and 1% penicillin/streptomycin and incubated at 37°C with 5% CO_2.

Construction of OVs

The BiTE molecule was constructed by linking a Claudin18.2-targeting scFv to a CD3ε-targeting scFv with glycine-serine (G4S) linkers. An IL-2 signal sequence and a His-tag sequence were added at the 5′ and 3′ ends of the BiTE gene. The GFP or IL2-BiTE-His-tag expression cassettes were inserted into the ICP34.5 location of the virus genome to construct OV-GFP and OV-BiTE. The viruses were propagated, tittered, and purified as previously described.[31] The safety of OV-BiTE in mice, especially liver and kidney toxicity, was assessed by both histological analysis of liver and kidney and biochemical test of blood.

Western blotting

Approximately 1×10^6 Vero cells were infected with OV at a multiplicity of infection (MOI) of 1 and the supernatant was collected 48 h post infection and incubated with nickel nitrilotriacetic acid (Ni-NTA) resin at 4°C for 2 h, followed by washing with 20 mM imidazole. The resins were mixed with electrophoresis loading buffer and heated in boiling water for 5–10 min. The samples were subjected to SDS-polyacrylamide gel electrophoresis (PAGE) and transferred onto polyvinylidene difluoride (PVDF) membranes. The His-tag BiTE on the membrane was probed using the anti-His-tag antibody (66005-1, Proteintech).

Cell proliferation assay

Approximately 2×10^4 cells were mixed with OV at an MOI of 1. After 24 h, the cell culture medium was removed and 1×10^5 PBMCs were added to each well. The number of tumor cells was determined using CCK8 (C6005; UE, Soochow, PR China) at different time points post infection.

ATP release detection

Approximately 2×10^5 cells were mixed with OV at an MOI of 1 and 1×10^6 PBMCs were added to each well. After 48 h, the supernatant was collected to detect ATP concentration using the Enhanced ATP Assay Kit (S0027, Beyotime).

Reporter cells assay

Approximately 1×10^6 cells were mixed with OV at an MOI of 1. Twenty-four hours post infection, and the infected tumor cells were mixed with 5×10^6 Jurkat-pIL2-GFP reporter cells for 24-h co-culture.[32] The reporter Jurkat cells were harvested and subjected to flow cytometry analysis to detect the expression of GFP.

Detection of IFN-γ and IL-2 secretion

Approximately 2×10^4 cells were mixed with OV at an MOI of 1. After 24 h, 1×10^5 PBMCs were added to each well. After 48 h, the supernatant was harvested and the level of cytokine was detected using the Human IFN-γ Valukine ELISA Kit (VAL104, Novus Bio) and Human IL-2 ELISA Set (555190, BD Biosciences).

Mouse model

The NOD-*Prkdc*^{scid} *Il2rg*^{em1}*/Smoc* (M-NSG) and C57BL/6-*Cd3e*$^{em1(hCD3E)\ Smoc}$ (CD3E-HU) were obtained from the Shanghai Model Organisms Center (Shanghai, PR China).

For the xenograft mouse model, 5×10^6 DAN-G cells were subcutaneously implanted into the right flank of 6-week-old male NSG mice. When the tumor volumes reached 80–120 mm^3, the tumor-bearing mice were intravenously injected with 1×10^7 human PBMCs through the tail vein (set as day 0). Approximately 1×10^6 plaque-forming units (PFU) of purified OVs were intratumorally injected on days 3, 6, and 9, respectively.

For the KPC syngeneic tumor mouse model, approximately 5×10^6 KPC-hClaudin18.2 cells were mixed with Matrigel (v/v = 1:1) and subcutaneously implanted into the right flank of 6-week-old male CD3E-HU mice. Once the tumor volumes reached 100–120 mm^3 (day 0), the tumor-bearing mice were intratumorally treated with 1×10^6 PFU of purified OVs per mouse on days 0, 3, 6, 9, and 12.

For the Pan02 syngeneic tumor mouse model, approximately 5×10^5 Pan02-HVEM-hClaudin18.2 cells were mixed with Matrigel (v/v = 1:1) and subcutaneously implanted into the right flank of 6-week-old male

CD3E-HU mice. Once the tumor volumes reached 60–100 mm^3 (day 0), the tumor-bearing mice were intratumorally treated with 2×10^6 PFU of purified OVs per mouse on days 0, 3, and 6.

Tumor length and width were measured three times per week using a digital caliper, and tumor volumes (V, mm^3) were calculated using the formula $0.5 \times (\text{length} \times \text{width}2)$. Mice were euthanized when the tumor volume reached 2,000 mm^3. The survival of tumor-bearing mice was monitored and analyzed using Kaplan-Meier curves.

Flow cytometry analysis

The mice were sacrificed 3 days after the last treatment. Tumor tissues were collected and cut into pieces. The single-cell suspension was prepared by using dissociation buffer (1 mg/mL collagenase IV, 1 mg/mL hyaluronidase, and 20 U/mL DNase in PBS plus 2% FBS). The red blood cells were removed by incubating with ammonium-chloride-potassium (ACK) lysis buffer (CS0001, Leagene). The dissociated cells were resuspended in 30% Percoll and concentrated at $400 \times g$ for 10 min. The single-cell suspension was stained with Zombie NIR Fixable Viability Kit (423105, BioLegend) and fluorescence-conjugated antibodies. Flow cytometry analysis was performed on an LSR Fortessa flow cytometer (BD Biosciences), and data were processed using FlowJo v10 software (TreeStar, USA).

Tumor-killing effects of TAMs

To evaluate and compare the tumor-killing potential of TAMs from KPC mice treated with OV-GFP or OV-BiTE, TAMs were isolated from the tumors of treated mice using F4/80 magnetic beads (130-110-443, Miltenyi), while splenocytes from a freshly sacrificed mouse served as effector cells. KPC-Claudin18.2 target cells were seeded in 96-well plates and co-cultured with TAMs and splenocytes at a 1:5:1 ratio for 3 days. After washing off suspended cells, CCK-8 reagent were added to measure absorbance at 450 nm.

Immunohistochemistry and picrosirius red staining

Three days after the last OV treatment, tumor-bearing mice were euthanized. Tumor samples were fixed with 4% paraformaldehyde at 4°C for 24 h, embedded in paraffin, and serially cut into 8-μm sections. The sections were stained with antibodies and picrosirius red with Picrosirius Red Stain Kit (BP-DL030, Sbjbio).

MIHC

The mIHC was performed using AlphaTSA Multiplex IHC Kit (AXT37100031, Alphaxbio) according to the manufacturer's instructions. Briefly, the paraffin sections were dewaxed and hydrated through a series of xylene-to-alcohol washes followed by antigen repair and sealing. Then, the slides were blocked and incubated with primary antibodies, followed by secondary antibodies. Fluorescence staining was then performed. Finally, the slides were stained with DAPI.

Viral DNA copy number quantification

Mice were sacrificed at day 13 (1 day after the last treatment) and day 16 (4 days after the last treatment). Spleen, liver, lung, kidney, and tumor tissues were harvested and homogenized. Genomic DNA was extracted using a commercial kit (D1700, Solarbio). HSV glycoprotein D (gD) gene copies in the extracted DNA were quantified by qPCR using the following primers:

gD forward: 5′-TACAACCTGACCATCGCTTG-3′

gD reverse: 5′-GCCCCCAGAGACTTGTTGTA-3′

Statistical analysis

Quantitative data were presented as the mean ± standard error of the mean (SEM) of at least three independent experiments. Data were analyzed using one-way analysis of variance (ANOVA) with Dunnett tests or two-way ANOVA with Sidak's tests. Animal survival was plotted using Kaplan-Meier curves and compared using the log rank test. A p value less than 0.05 was considered to be statistically significant (*$p < 0.05$, **$p < 0.01$, ***$p < 0.001$, and ****$p < 0.0001$).

DATA AND CODE AVAILABILITY

Data are available on reasonable request.

SUPPLEMENTAL INFORMATION

Supplemental information can be found online at https://doi.org/10.1016/j.omto.2023.08.011.

ACKNOWLEDGMENTS

All animal experiments in this study were approved by the Institute Research Ethics Committee of Nankai University, Tianjin, China (2021-SYDWLL-000125).

This work was supported by the National Natural Science Foundation of China (grant numbers 82261138553 and 32171468), the Fundamental Research Funds for the Central Universities, Nankai University (grant numbers 63223035 and ZB19100123), the Medical Talent Project of Tianjin City (TJSJMYXYC-D2-032), Key Research Fund of Tianjin Project and Team (XB202010), Key Research and Development Program of Tianjin (20YFZCSY00450), and Tianjin Key Medical Discipline (Specialty) Construction Project (TJYXZDXK-048A).

AUTHOR CONTRIBUTIONS

M.D., H.Z., M.Z., and Y.Y. designed experiments and analyzed the data. S.L., F.L., and L.D. performed the experiments. Q.M., W.L., Z.Z., H.L., Y.Z., M.H., and H.W. provided some of the experiment resources and technical support. All authors contributed to the writing and reviewing of the manuscript.

DECLARATION OF INTERESTS

The authors declare no competing interests.

REFERENCES

1. Sung, H., Ferlay, J., Siegel, R.L., Laversanne, M., Soerjomataram, I., Jemal, A., and Bray, F. (2021). Global cancer statistics 2020: GLOBOCAN estimates of incidence and mortality worldwide for 36 cancers in 185 countries. CA. Cancer J. Clin. *71*, 209–249. https://doi.org/10.3322/caac.21660.

2. Siegel, R.L., Miller, K.D., and Jemal, A. (2020). Cancer statistics, 2020. CA. Cancer J. Clin. *70*, 7–30. https://doi.org/10.3322/caac.21590.

3. Sarantis, P., Koustas, E., Papadimitropoulou, A., Papavassiliou, A.G., and Karamouzis, M.V. (2020). Pancreatic ductal adenocarcinoma: Treatment hurdles, tumor microenvironment and immunotherapy. World J. Gastrointest. Oncol. *12*, 173–181. https://doi.org/10.4251/wjgo.v12.i2.173.

4. Yoon, J.H., Jung, Y.J., and Moon, S.H. (2021). Immunotherapy for pancreatic cancer. World J. Clin. Cases *9*, 2969–2982. https://doi.org/10.12998/wjcc.v9.i13.2969.

5. Singh, P., Toom, S., and Huang, Y. (2017). Anti-claudin 18.2 antibody as new targeted therapy for advanced gastric cancer. J. Hematol. Oncol. *10*, 105. https://doi.org/10.1186/s13045-017-0473-4.

6. Wöll, S., Schlitter, A.M., Dhaene, K., Roller, M., Esposito, I., Sahin, U., and Türeci, Ö. (2014). Claudin 18.2 is a target for IMAB362 antibody in pancreatic neoplasms. Int. J. Cancer *134*, 731–739. https://doi.org/10.1002/ijc.28400.

7. Zhu, G., Foletti, D., Liu, X., Ding, S., Melton Witt, J., Hasa-Moreno, A., Rickert, M., Holz, C., Aschenbrenner, L., Yang, A.H., et al. (2019). Targeting CLDN18.2 by CD3 Bispecific and ADC Modalities for the Treatments of Gastric and Pancreatic Cancer. Sci. Rep. *9*, 8420. https://doi.org/10.1038/s41598-019-44874-0.

8. Sahin, U., Türeci, Ö., Manikhas, G., Lordick, F., Rusyn, A., Vynnychenko, I., Dudov, A., Bazin, I., Bondarenko, I., Melichar, B., et al. (2021). FAST: a randomised phase II study of zolbetuximab (IMAB362) plus EOX versus EOX alone for first-line treatment of advanced CLDN18.2-positive gastric and gastro-oesophageal adenocarcinoma. Ann. Oncol. *32*, 609–619. https://doi.org/10.1016/j.annonc.2021.02.005.

9. Middelburg, J., Kemper, K., Engelberts, P., Labrijn, A.F., Schuurman, J., and van Hall, T. (2021). Overcoming Challenges for CD3-Bispecific Antibody Therapy in Solid Tumors. Cancers (Basel) *13*, 287. https://doi.org/10.3390/cancers13020287.

10. Zuo, S., Wei, M., Xu, T., Kong, L., He, B., Wang, S., Wang, S., Wu, J., Dong, J., and Wei, J. (2021). An engineered oncolytic vaccinia virus encoding a single-chain variable fragment against TIGIT induces effective antitumor immunity and synergizes with PD-1 or LAG-3 blockade. J. Immunother. Cancer *9*, e002843. https://doi.org/10.1136/jitc-2021-002843.

11. Wang, G., Kang, X., Chen, K.S., Jehng, T., Jones, L., Chen, J., Huang, X.F., and Chen, S.Y. (2020). An engineered oncolytic virus expressing PD-L1 inhibitors activates tumor neoantigen-specific T cell responses. Nat. Commun. *11*, 1395. https://doi.org/10.1038/s41467-020-15229-5.

12. Huang, J.K., Ma, L., Song, W.H., Lu, B.Y., Huang, Y.B., Dong, H.M., Ma, X.K., Zhu, Z.Z., and Zhou, R. (2016). MALAT1 promotes the proliferation and invasion of thyroid cancer cells via regulating the expression of IQGAP1. Biomed. Pharmacother. *83*, 1–7. https://doi.org/10.1016/j.biopha.2016.05.039.

13. Porter, C.E., Rosewell Shaw, A., Jung, Y., Yip, T., Castro, P.D., Sandulache, V.C., Sikora, A., Gottschalk, S., Ittman, M.M., Brenner, M.K., and Suzuki, M. (2020). Oncolytic Adenovirus Armed with BiTE, Cytokine, and Checkpoint Inhibitor Enables CAR T Cells to Control the Growth of Heterogeneous Tumors. Mol. Ther. *28*, 1251–1262. https://doi.org/10.1016/j.ymthe.2020.02.016.

14. Freedman, J.D., Hagel, J., Scott, E.M., Psallidas, I., Gupta, A., Spiers, L., Miller, P., Kanellakis, N., Ashfield, R., Fisher, K.D., et al. (2017). Oncolytic adenovirus expressing bispecific antibody targets T-cell cytotoxicity in cancer biopsies. EMBO Mol. Med. *9*, 1067–1087. https://doi.org/10.15252/emmm.201707567.

15. Khalique, H., Baugh, R., Dyer, A., Scott, E.M., Frost, S., Larkin, S., Lei-Rossmann, J., and Seymour, L.W. (2021). Oncolytic herpesvirus expressing PD-L1 BiTE for cancer therapy: exploiting tumor immune suppression as an opportunity for targeted immunotherapy. J. Immunother. Cancer *9*, e001292. https://doi.org/10.1136/jitc-2020-001292.

16. Rahal, A., and Musher, B. (2017). Oncolytic viral therapy for pancreatic cancer. J. Surg. Oncol. *116*, 94–103. https://doi.org/10.1002/jso.24626.

17. Santos Apolonio, J., Lima de Souza Gonçalves, V., Cordeiro Santos, M.L., Silva Luz, M., Silva Souza, J.V., Rocha Pinheiro, S.L., de Souza, W.R., Sande Loureiro, M., and de Melo, F.F. (2021). Oncolytic virus therapy in cancer: A current review. World J. Virol. *10*, 229–255. https://doi.org/10.5501/wjv.v10.i5.229.

18. Andtbacka, R.H.I., Kaufman, H.L., Collichio, F., Amatruda, T., Senzer, N., Chesney, J., Delman, K.A., Spitler, L.E., Puzanov, I., Agarwala, S.S., et al. (2015). Talimogene Laherparepvec Improves Durable Response Rate in Patients With Advanced Melanoma. J. Clin. Oncol. *33*, 2780–2788. https://doi.org/10.1200/jco.2014.58.3377.

19. Taylor, I.P., and Lopez, J.A. (2023). Oncolytic adenoviruses and the treatment of pancreatic cancer: a review of clinical trials. J. Cancer Res. Clin. Oncol. *149*, 8117–8129. https://doi.org/10.1007/s00432-023-04735-w.

20. Musher, B.L., Smaglo, B.G., Abidi, W., Othman, M., Patel, K., Jawaid, S., Jing, J., Brisco, A., Wenthe, J., Eriksson, E., et al. (2022). A phase I/II study of LOAd703, a TMZ-CD40L/4-1BBL-armed oncolytic adenovirus, combined with nab-paclitaxel and gemcitabine in advanced pancreatic cancer. J. Clin. Oncol. *40*, 4138. https://doi.org/10.1200/JCO.2022.40.16_suppl.4138.

21. Ariston Gabriel, A.N., Jiao, Q., Yvette, U., Yang, X., Al-Ameri, S.A., Du, L., Wang, Y.S., and Wang, C. (2020). Differences between KC and KPC pancreatic ductal adenocarcinoma mice models, in terms of their modeling biology and their clinical relevance. Pancreatology *20*, 79–88. https://doi.org/10.1016/j.pan.2019.11.006.

22. Lee, J.W., Komar, C.A., Bengsch, F., Graham, K., and Beatty, G.L. (2016). Genetically Engineered Mouse Models of Pancreatic Cancer: The KPC Model (LSL-Kras(G12D/+) ;LSL-Trp53(R172H/+) ;Pdx-1-Cre), Its Variants, and Their Application in Immuno-oncology Drug Discovery. Curr. Protoc. Pharmacol. *73*, 14.39.11–14.39.20. https://doi.org/10.1002/cpph.2.

23. Zhang, L., Wang, W., Wang, R., Zhang, N., Shang, H., Bi, Y., Chen, D., Zhang, C., Li, L., Yin, J., et al. (2021). Reshaping the Immune Microenvironment by Oncolytic Herpes Simplex Virus in Murine Pancreatic Ductal Adenocarcinoma. Mol. Ther. *29*, 744–761. https://doi.org/10.1016/j.ymthe.2020.10.027.

24. Yu, F., Wang, X., Guo, Z.S., Bartlett, D.L., Gottschalk, S.M., and Song, X.T. (2014). T-cell engager-armed oncolytic vaccinia virus significantly enhances antitumor therapy. Mol. Ther. *22*, 102–111. https://doi.org/10.1038/mt.2013.240.

25. Speck, T., Heidbuechel, J.P.W., Veinalde, R., Jaeger, D., von Kalle, C., Ball, C.R., Ungerechts, G., and Engeland, C.E. (2018). Targeted BiTE Expression by an Oncolytic Vector Augments Therapeutic Efficacy Against Solid Tumors. Clin. Cancer Res. *24*, 2128–2137. https://doi.org/10.1158/1078-0432.CCR-17-2651.

26. Engeland, C.E., Grossardt, C., Veinalde, R., Bossow, S., Lutz, D., Kaufmann, J.K., Shevchenko, I., Umansky, V., Nettelbeck, D.M., Weichert, W., et al. (2014). CTLA-4 and PD-L1 checkpoint blockade enhances oncolytic measles virus therapy. Mol. Ther. *22*, 1949–1959. https://doi.org/10.1038/mt.2014.160.

27. Veinalde, R., Grossardt, C., Hartmann, L., Bourgeois-Daigneault, M.C., Bell, J.C., Jäger, D., von Kalle, C., Ungerechts, G., and Engeland, C.E. (2017). Oncolytic measles virus encoding interleukin-12 mediates potent antitumor effects through T cell activation. Oncoimmunology *6*, e1285992. https://doi.org/10.1080/2162402X.2017.1285992.

28. Wing, A., Fajardo, C.A., Posey, A.D., Jr., Shaw, C., Da, T., Young, R.M., Alemany, R., June, C.H., and Guedan, S. (2018). Improving CART-Cell Therapy of Solid Tumors with Oncolytic Virus-Driven Production of a Bispecific T-cell Engager. Cancer Immunol. Res. *6*, 605–616. https://doi.org/10.1158/2326-6066.CIR-17-0314.

29. Freedman, J.D., Duffy, M.R., Lei-Rossmann, J., Muntzer, A., Scott, E.M., Hagel, J., Campo, L., Bryant, R.J., Verrill, C., Lambert, A., et al. (2018). An Oncolytic Virus Expressing a T-cell Engager Simultaneously Targets Cancer and Immunosuppressive Stromal Cells. Cancer Res. *78*, 6852–6865. https://doi.org/10.1158/0008-5472.CAN-18-1750.

30. Heidbuechel, J.P.W., and Engeland, C.E. (2021). Oncolytic viruses encoding bispecific T cell engagers: a blueprint for emerging immunovirotherapies. J. Hematol. Oncol. *14*, 63. https://doi.org/10.1186/s13045-021-01075-5.

31. Wang, R., Chen, J., Wang, W., Zhao, Z., Wang, H., Liu, S., Li, F., Wan, Y., Yin, J., Wang, R., et al. (2022). CD40L-armed oncolytic herpes simplex virus suppresses pancreatic ductal adenocarcinoma by facilitating the tumor microenvironment favorable to cytotoxic T cell response in the syngeneic mouse model. J. Immunother. Cancer *10*, e003809. https://doi.org/10.1136/jitc-2021-003809.

32. Wang, Y., Jin, R., Shen, B., Li, N., Zhou, H., Wang, W., Zhao, Y., Huang, M., Fang, P., Wang, S., et al. (2021). High-throughput functional screening for next-generation cancer immunotherapy using droplet-based microfluidics. Sci. Adv. *7*, eabe3839. https://doi.org/10.1126/sciadv.abe3839.